Performance of GaN-based light-emitting diodes fabricated using GaN epilayers grown on silicon substrates

Ray-Hua Horng,[1,4*] Bing-Rui Wu,[1,2] Ching-Ho Tien,[2] Sin-Liang Ou,[2] Min-Hao Yang,[2] Hao-Chung Kuo,[5] and Dong-Sing Wuu[2,3]

[1]*Graduate Institute of Precision Engineering, National Chung Hsing University, Taichung 402, Taiwan*
[2]*Department of Materials Science and Engineering, National Chung Hsing University, Taichung 402, Taiwan*
[3]*Department of Materials Science and Engineering, Da-Yeh University, Changhua 515, Taiwan*
[4]*Advanced Optoelectronic Technology Center, National Cheng Kung University, Tainan 701, Taiwan*
[5]*Department of Photonics, National Chiao Tung University, Hsingchu 300, Taiwan*
[*]*huahorng@nchu.edu.tw*

Abstract: Light extraction of GaN-based light-emitting diodes grown on Si(111) substrate (GaN-on-Si based LEDs) is presented in this study. Three different designs of GaN-on-Si based LEDs with the lateral structure, lateral structure on mirror/Si(100) substrate, and vertical structure on mirror/Si(100) substrate were epitaxially grown by metalorganic chemical vapor deposition and fabricated using chemical lift-off and double-transfer techniques. Current-voltage, light output power, far-field radiation patterns, and electroluminescence characteristics of these three LEDs were discussed. At an injection current of 700 mA, the output powers of LEDs with the lateral structure on mirror/Si(100) substrate and vertical structure on mirror/Si(100) substrate were measured to be 155.07 and 261.07 mW, respectively. The output powers of these two LEDs had 70.63% and 187.26% enhancement compared to that of LED with the lateral structure, respectively. The result indicated this vertical structure LED was useful in improving the light extraction due to an enhancement in light scattering efficiency while the high-reflection mirror and diffuse surfaces were employed.

OCIS codes: (160.2100) Electro-optical materials; (230.3670) Light-emitting diodes.

References and links

1. P. Kung, D. Walker, M. Hamilton, J. Diaz, and M. Razeghi, "Lateral epitaxial overgrowth of GaN films on sapphire and silicon substrates," Appl. Phys. Lett. **74**(4), 570–572 (1999).
2. A. Watanabe, T. Takeuchi, K. Hirosawa, H. Amano, K. Hiramatsu, and I. Akasaki, "The growth of single crystalline GaN on a Si substrate using AIN as an intermediate layer," J. Cryst. Growth **128**(1–4), 391–396 (1993).
3. T. M. Katona, M. D. Craven, P. T. Fini, J. S. Speck, and S. P. DenBaars, "Observation of crystallographic wing tilt in cantilever epitaxy of GaN on silicon carbide and silicon (111) substrates," Appl. Phys. Lett. **79**(18), 2907–2909 (2001).
4. E. Feltin, B. Beaumont, M. Laugt, P. De Mierry, P. Vennegues, H. Lahreche, M. Leroux, and P. Gibart, "Stress control in GaN grown on silicon (111) by metalorganic vapor phase epitaxy," Appl. Phys. Lett. **79**(20), 3230–3232 (2001).
5. A. Dadgar, J. Bläsing, A. Diez, A. Alam, M. Heuken, and A. Krost, "Metalorganic chemical vapor phase epitaxy of crack-free GaN on Si (111) exceeding 1 μm in thickness," Jpn. J. Appl. Phys. **39**(Part 2, No. 11B 11B), L1183–L1185 (2000).
6. T. Egawa, B. Zhang, and H. Ishikawa, "High performance of InGaN LEDs on (111) silicon substrates grown by MOCVD," IEEE Electron Device Lett. **26**(3), 169–171 (2005).
7. H. Ishikawa, G. Zhao, N. Nakada, T. Egawa, T. Soga, T. Jimbo, and M. Umeno, "High-Quality GaN on Si Substrate Using AlGaN/AlN Intermediate Layer," Phys. Status Solidi A **176**(1), 599–603 (1999).
8. C. A. Tran, A. Osinski, R. F. Karlicek, and I. Berishev, "Growth of InGaN/GaN multiple-quantum-well blue light-emitting diodes on silicon by metalorganic vapor phase epitaxy," Appl. Phys. Lett. **75**(11), 1494–1496 (1999).

#202212 - $15.00 USD Received 28 Nov 2013; revised 3 Jan 2014; accepted 3 Jan 2014; published 10 Jan 2014

9. H. Lahrèche, P. Vennegues, O. Tottereau, M. Laügt, P. Lorenzini, M. Leroux, B. Beaumont, and P. Gibart, "Optimisation of AlN and GaN growth by metalorganic vapour-phase epitaxy (MOVPE) on Si (111)," J. Cryst. Growth **217**(1–2), 13–25 (2000).
10. S. Raghavan and J. M. Redwing, "Intrinsic stresses in AlN layers grown by metal organic chemical vapor deposition on (0001) sapphire and (111) Si substrates," J. Appl. Phys. **96**(5), 2995–3003 (2004).
11. C. Mo, W. Fang, Y. Pu, H. Liu, and F. Jiang, "Growth and characterization of InGaN blue LED structure on Si (111) by MOCVD," J. Cryst. Growth **285**(3), 312–317 (2005).
12. S. Guha and N. A. Bojarczuk, "Ultraviolet and violet GaN light emitting diodes on silicon," Appl. Phys. Lett. **72**(4), 415–417 (1998).
13. C. A. Tran, A. Osinski, R. Karlicek, and I. Berishev, "Growth of InGaN/GaN multiple-quantum-well blue light-emitting diodes on silicon by metalorganic vapor phase epitaxy," Appl. Phys. Lett. **75**(11), 1494–1496 (1999).
14. A. Dadgar, J. Christen, T. Riemann, S. Richter, J. Blasing, A. Diez, A. Krost, A. Alam, and M. Heuken, "Bright blue electroluminescence from an InGaN/GaN multiquantum-well diode on Si (111): Impact of an AlGaN/GaN multilayer," Appl. Phys. Lett. **78**(15), 2211–2213 (2001).
15. T. Egawa, T. Moku, H. Ishikawa, K. Ohtsuka, and T. Jimbo, "Improved characteristics of blue and green InGaN-based light-emitting diodes on Si grown by metalorganic chemical vapor deposition," Jpn. J. Appl. Phys. **41**(Part 2, No. 6B 6B), L663–L664 (2002).
16. R. Ravash, A. Dadgar, F. Bertram, A. Dempewolf, S. Metzner, T. Hempel, J. Christen, and A. Krost, "MOVPE growth of semi-polar GaN light-emitting diode structures on planar Si (112) and Si (113) substrates," J. Cryst. Growth **370**, 288–292 (2013).
17. Y. H. Ra, R. Navamathavan, J. H. Park, and C. R. Lee, "High-quality uniaxial $In_xGa_{1-x}N$/GaN multiple quantum well (MQW) nanowires (NWs) on Si (111) grown by metal-organic chemical vapor deposition (MOCVD) and light-emitting diode (LED) fabrication," ACS Appl. Mater. Interfaces **5**(6), 2111–2117 (2013).
18. C. Kisielowski, J. Krüger, S. Ruvimov, T. Suski, J. W. Ager 3rd, E. Jones, Z. Liliental-Weber, M. Rubin, E. R. Weber, M. D. Bremser, and R. F. Davis, "Strain-related phenomena in GaN thin films," Phys. Rev. B Condens. Matter **54**(24), 17745–17753 (1996).
19. V. Y. Davydov, Y. E. Kitaev, I. N. Goncharuk, A. N. Smirnov, J. Graul, O. Semchinova, D. Uffmann, M. Smirnov, A. Mirgorodsky, and R. Evarestov, "Phonon dispersion and Raman scattering in hexagonal GaN and AlN," Phys. Rev. B **58**(19), 12899–12907 (1998).
20. S. Tripathy, S. J. Chua, P. Chen, and Z. L. Miao, "Micro-Raman investigation of strain in GaN and $Al_xGa_{1-x}N$/GaN heterostructures grown on Si (111)," J. Appl. Phys. **92**(7), 3503–3510 (2002).
21. T. Kozawa, T. Kachi, H. Kano, H. Nagase, N. Koide, and K. Manabe, "Thermal stress in GaN epitaxial layers grown on sapphire substrates," J. Appl. Phys. **77**(9), 4389–4392 (1995).
22. S. J. Lee, K. H. Kim, J. W. Ju, T. Jeong, C.-R. Lee, and J. H. Baek, "High-brightness GaN-based light-emitting diodes on Si using wafer bonding technology," Appl. Phys. Express **4**(6), 066501 (2011).
23. S. C. Hsu, B. J. Pong, W. H. Li, T. E. Beechem III, S. Graham, and C. Y. Liu, "Stress relaxation in GaN by transfer bonding on Si substrates," Appl. Phys. Lett. **91**(25), 251114 (2007).
24. T. Kuroda and A. Tackeuchi, "Influence of free carrier screening on the luminescence energy shift and carrier lifetime of InGaN quantum wells," J. Appl. Phys. **92**(6), 3071–3074 (2002).
25. C. Wang, S. Chang, W. Chang, J. Li, Y. Lu, Z. Li, H. Yang, H. Kuo, T. Lu, and S. Wang, "Efficiency droop alleviation in InGaN/GaN light-emitting diodes by graded-thickness multiple quantum wells," Appl. Phys. Lett. **97**(18), 181101 (2010).
26. T. Takeuchi, S. Sota, M. Katsuragawa, M. Komori, H. Takeuchi, H. Amano, and I. Akasaki, "Quantum-confined Stark effect due to piezoelectric fields in GaInN strained quantum wells," Jpn. J. Appl. Phys. **36**(Part 2, No. 4A 4A), L382–L385 (1997).
27. J. H. Ryou, P. D. Yoder, J. Liu, Z. Lochner, H. Kim, S. Choi, H. J. Kim, and R. D. Dupuis, "Control of quantum-confined stark effect in InGaN-based quantum wells," IEEE J. Sel. Top. Quantum Electron. **15**(4), 1080–1091 (2009).
28. S. J. Wang, K. M. Uang, S. L. Chen, Y. C. Yang, S. C. Chang, T. M. Chen, C. H. Chen, and B. W. Liou, "Use of patterned laser liftoff process and electroplating nickel layer for the fabrication of vertical-structured GaN-based light-emitting diodes," Appl. Phys. Lett. **87**(1), 011111 (2005).
29. H. W. Jang, S. W. Ryu, H. K. Yu, S. Lee, and J.-L. Lee, "The role of reflective p-contacts in the enhancement of light extraction in nanotextured vertical InGaN light-emitting diodes," Nanotechnology **21**(2), 025203 (2010).
30. T. Fujii, Y. Gao, R. Sharma, E. Hu, S. DenBaars, and S. Nakamura, "Increase in the extraction efficiency of GaN-based light-emitting diodes via surface roughening," Appl. Phys. Lett. **84**(6), 855–857 (2004).
31. C. Huh, K. S. Lee, E. J. Kang, and S. J. Park, "Improved light-output and electrical performance of InGaN-based light-emitting diode by microroughening of the p-GaN surface," J. Appl. Phys. **93**(11), 9383–9385 (2003).
32. J. Piprek, "Efficiency droop in nitride-based light-emitting diodes," Phys. Status Solidi A **207**(10), 2217–2225 (2010).
33. E. Kioupakis, P. Rinke, K. T. Delaney, and C. G. Van de Walle, "Indirect Auger recombination as a cause of efficiency droop in nitride light-emitting diodes," Appl. Phys. Lett. **98**(16), 161107 (2011).
34. J. Xie, X. Ni, Q. Fan, R. Shimada, U. Ozgur, and H. Morkoç, "On the efficiency droop in InGaN multiple quantum well blue light emitting diodes and its reduction with p-doped quantum well barriers," Appl. Phys. Lett. **93**(12), 121107 (2008).

#202212 - $15.00 USD Received 28 Nov 2013; revised 3 Jan 2014; accepted 3 Jan 2014; published 10 Jan 2014

35. M. H. Kim, M. F. Schubert, Q. Dai, J. K. Kim, E. F. Schubert, J. Piprek, and Y. Park, "Origin of efficiency droop in GaN-based light-emitting diodes," Appl. Phys. Lett. **91**(18), 183507 (2007).

1. Introduction

GaN-based light-emitting diodes grown on silicon substrate (GaN-on-Si based LEDs) are thought to be one of the most promising choices for high power LEDs applications owing to the numerous advantages of Si substrate, such as low manufacturing cost, good thermal and electrical conductivities, large scale availability with high quality, and the possibility of integration for Si electronics on the same chip [1–4]. Moreover, the high conductivity of Si substrate provides a chance to form ohmic contacts directly on the backside, which makes an easier LED fabrication technique than the traditional process on sapphire substrate.

In general, GaN-on-Si growth is usually performed by using chemical vapor deposition, pulsed laser deposition, and metalorganic chemical vapor deposition (MOCVD). However, it is difficult to grow high-performance GaN-based LEDs on Si substrates (typical Si(111) wafer) due to the both large mismatches of the lattice constant (16.9%) and the thermal expansion coefficient (57%) between GaN and Si [2]. Additionally, the cracks are easily created when the thickness of GaN epilayer exceeds the critical value around 1 μm [5, 6].

To solve these problems, several intensive researches have been dedicated to the optimization for the epitaxial growth of GaN-on-Si, especially for the stress management and crack reduction in the epilayer [2–4, 7–11]. Among these approaches, the employment of nucleation buffer layers [e.g. aluminum nitride (AlN) or aluminum gallium nitride ($Al_xGa_{1-x}N$) graded layers] on Si substrates is a prospective technique to counterbalance the thermally induced tensile strains for subsequent growth of crack-free GaN epilayers. Furthermore, GaN-based LEDs are also successfully fabricated on Si substrates [12–17].

On the other hand, the electrical and optical performances of the GaN-based LEDs on Si substrates are both poorer than those on sapphire. This can be explained by two reasons. Firstly, owing to the formation of tensile stress in thin GaN layer resulted from the thermal expansion mismatch between GaN and Si, an introduction of highly resistant AlN (or AlGaN) layer is required, which will induce the high voltage in the lateral-electrode device applications. Secondly, optical loss of the downward light is another difficulty in achieving high performance LEDs by using the opaque Si substrate.

In this study, to solve the problem of downward light absorption, two kinds of GaN-on-Si LEDs are fabricated. One is the lateral structure GaN-on-Si based LEDs prepared by the double-transfer techniques consisting of wafer bonding process, high-reflection mirror, and chemical lift-off (CLO) process. The other one is the vertical structure GaN-on-Si based LEDs with a high-reflection mirror by wafer bonding, CLO process, and n-GaN surface texturization to achieve high-performance and high-brightness LEDs. In particular, we demonstrate greatly improved optical and electrical properties of the lateral-type GaN-based LEDs on mirror/Si(100) substrate and vertical-type GaN-based LEDs on mirror/Si(100) substrate compared with the original lateral devices.

2. Experimental

GaN-on-Si based LED epilayers used in this study were grown by MOCVD. From the Si(111) substrate to the top surface, the LED epilayers consisted of a 0.2-μm-thick AlN buffer layer, a 1.2-μm-thick graded AlGaN buffer layer, a 1-μm-thick undoped GaN layer (u-GaN), and a 2-μm-thick Si-doped n-GaN layer, ten periods of InGaN/GaN multiple-quantum-well (MQW) active layers, and a 0.1-μm-thick Mg-doped p-GaN layer. After growth, a thermal annealing process was performed on the epitaxial wafers to activate the p-type layer at 850 °C for 30 min. Three kinds of LED configurations were considered in this study. One is fabricated as the lateral structure GaN-on-Si based LED (denoted as LS-LED), another is the lateral structure GaN-based LED on mirror/Si(100) substrate by using double-transfer process (denoted as DT-LED), and the other is the vertical structure GaN-based LED on mirror/Si(100) substrate

#202212 - $15.00 USD Received 28 Nov 2013; revised 3 Jan 2014; accepted 3 Jan 2014; published 10 Jan 2014

(denoted as VS-LED), as schematically shown in Fig. 1. For the device process, one LED chip was defined with the size of 40 mil × 40 mil. The LS-LED shown in Fig. 1(a) was fabricated using a standard photolithography process and dry etching technique. Indium tin oxide (ITO) transparent conductive layer and Cr/Au metal were deposited on the p-type and n-type GaN as the ohmic contacts, respectively. The DT-LED was transferred to Si(100) substrate by using double-transfer process to insert a high-reflection mirror. The as-prepared device was bonded to a glass carrier using temporary bonding material and then subjected to a CLO process. After immersing the entire LED device into the Si etchant (HNO_3: HF: $NaClO_2$), the Si(111) substrate was separated from the LED structure. Then, the epilayer with a micropillar surface was etched by inductively coupled plasma (ICP) to remove the residual AlN buffer layer on the u-GaN. In order to further achieve higher extraction efficiency, the u-GaN was etched using NaOH with 4M concentration at 80 °C for 5 min. Immediately, the silicon-removed LEDs with a single-side roughened u-GaN surface was bonded to a Si(100) carrier with the Ni/Ag mirror as a permanent substrate, followed by the removal of the glass carrier. Finally, a p-side-up GaN on mirror/Si(100) substrate was obtained, as shown in Fig. 1(b). Figure 1(c) shows a schematic structure of the VS-LED, which was a vertical-type GaN-on-Si based LEDs on mirror/Si(100) substrate. Before the wafer bonding process, ITO/Ni/Ag and Au/In multilayers were deposited for the p-type ohmic contact, reflection and bonding metal layers, respectively. The GaN-based LEDs grown on Si(111) substrate was bonded to the Ag/Au/Cr deposited on (100)-oriented Si substrate by thermal-pressure bonding for 1 hour at 220 °C. Then, the Si(111) substrate, AlN buffer layer, and u-GaN layer were removed using the CLO process, ICP dry etching, and H_3PO_4 etching (130 °C, 6 min), respectively. To enable the n-contact formation, the roughened n-GaN surface was obtained by KOH etching treatment, where the surface presented a pyramidal pattern. Finally, Ti/Al/Ti/Au and Ti/Au metals were deposited on the textured n-GaN surface and the back surface of the Si substrate, respectively, to obtain the ohmic contacts. All LED chips were bonded onto a lead-frame to determine the current-voltage (I-V) characteristics. I-V measurement was carried out using an Agilent 4156 semiconductor parameter analyzer. The Raman spectrum was measured using a 488 nm argon-ion laser with a monochromator (Horiba Jobin-Yvon LabRam HR800 UV-vis μ-Raman). The light output power and electroluminescence (EL) spectra of these packaged LEDs were characterized by using an integrated sphere with a calibrated power meter (CAS 140B, Instrument Systems).

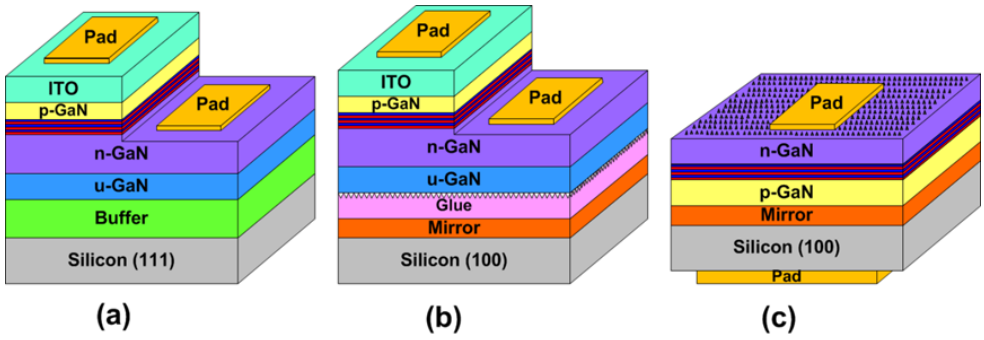

Fig. 1. Schematic diagrams of three kinds of GaN-on-Si based LED structure: (a) LS-LED (lateral structure without mirror), (b) DT-LED (lateral structure with mirror), and (c) VS-LED (vertical structure).

3. Result and discussion

LS-LED, DT-LED, and VS-LED present different electrical and optical properties even though they have the same GaN-on-Si epilayer structure. These differences result from the final design of device structure and the stress in epilayers after the transferring process. It is important to evaluate these devices performances. The typical I-V characteristics of these three GaN-on-Si based LEDs measured under the forward and reverse biases are shown in Figs. 2(a) and 2(b),

#202212 - $15.00 USD Received 28 Nov 2013; revised 3 Jan 2014; accepted 3 Jan 2014; published 10 Jan 2014

respectively. The forward voltages at an injection current of 350 mA for VS-LED, DT-LED, and LS-LED are observed as 3.6, 4.1, and 4.4 V, respectively. These I-V slopes show that the VS-LED has a slightly lower series resistance of 2.24 Ω compared to that of LS-LED (3.86 Ω) and DT-LED (3.14 Ω). It could be noted that the VS-LED presents a relatively lower current crowding effect due to its vertical design. This result reveals the VS-LED fabricated by the CLO process can provide better electrical properties than those of lateral structure LEDs. As shown in Fig. 2(b), the I-V characteristics measured under the reverse bias indicate that the leakage currents (@ −5 V) of VS-LED, DT-LED, and LS-LED are 1.2×10^{-6}, 3.3×10^{-6}, and 3.5×10^{-6} A, respectively. Obviously, the VS-LED still possesses a better reverse-biased I-V characteristic than that of the others. In addition, the parallel resistances of these three LEDs are calculated to be 16.7, 2.27 and 2.08 MΩ, respectively.

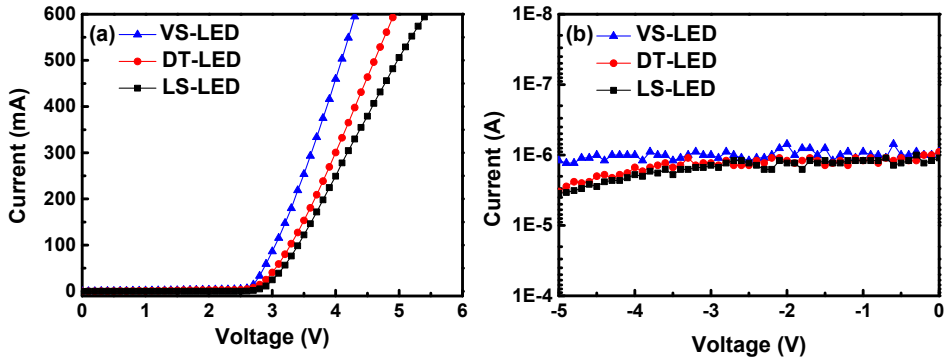

Fig. 2. I-V characteristics of the LS-LED, DT-LED, and VS-LED measured under the (a) forward and (b) reverse biases.

It is well known that there usually exists a large tensile stress in GaN epilayers grown on Si substrate due to the large difference in thermal expansion coefficient between GaN and Si. In this study, Raman spectra are measured to analyze the stress state of epilayers. Raman spectra are dominated by the E_2 (TO)-high mode phonons of LS-LED, DT-LED, and VS-LED at 564.32, 568.88, and 568.85 cm^{-1}, respectively, as shown in Fig. 3. According to previous researches, a 400-μm-thick freestanding GaN epilayer grown by hydride vapor phase epitaxy technique is assumed to be strain-free and the E_2 (TO) phonon is observed near 567.5 cm^{-1} [18–20]. This phonon wavenumber of 567.5 cm^{-1} is used as the reference value to determine the stress change of GaN epilayer. There are significant shifts of E_2 (high) phonon peak in these three LEDs. Based on the result reported by Kozawa et al., there is an empirical formula developed to estimate the stress levels of the GaN epilayer from Raman shift: $\Delta\omega = 6.2\sigma_{GaN}$, where $\Delta\omega$ is the strain-induced shift of the E_2 (high) phonon peak, σ_{GaN} is the in-plane biaxial stress, and 6.2 cm^{-1}/GPa for the E_2 (high) mode of GaN is the stress coefficient [21]. After calculation, it can be found that the LS-LED presented a compressive stress in GaN epilayers, which is estimated to be 0.51 GPa. The tensile stresses for VS-LED and DT-LED are estimated to be 0.217 and 0.223 GPa, respectively. Obviously, the epilayer transfer process can relax the epilayer stress (resulted from the MOCVD growth) after removing the Si substrate [22]. Moreover, the DT-LED shows more tensile stress because of the glue bonding using the twice epilayer transferring. In contrast with LS-LED, the red-shift of the VS-LED and DT-LED is observed, which indicates there is a relaxation of the compressive stress in the GaN epilayer after the transfer process. Consequently, the thermoelastic stress in GaN-on-Si LED devices can be controlled through the transfer process and could lead to an improvement in device performance and efficiency [22, 23].

#202212 - $15.00 USD Received 28 Nov 2013; revised 3 Jan 2014; accepted 3 Jan 2014; published 10 Jan 2014

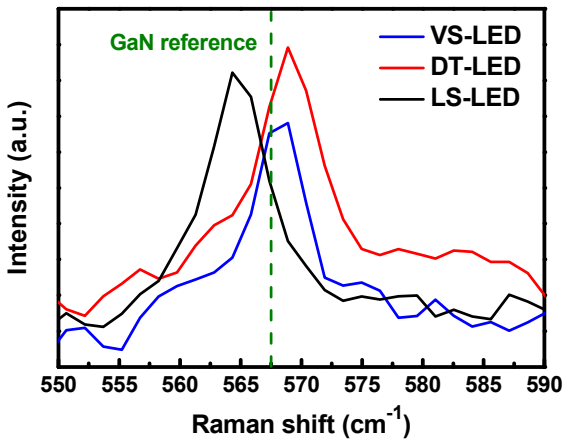

Fig. 3. Raman spectra of the LS-LED, DT-LED, and VS-LED.

As concerned the stress relaxation of epilayer in the GaN-based LEDs, it can be demonstrated from the EL spectra. Figure 4 shows the EL emission peak wavelength as a function of injection current for the LS-LED, DT-LED, and VS-LED at room temperature. Clearly, the result indicates that the VS-LED and DT-LED show longer EL wavelength than that of LS-LED at the injection current from 20 to 700 mA. It means that there is a red shift for the VS-LED and DT-LED. Peak wavelengths of LS-LED, VS-LED, and DT-LED at an injection current of 20 mA are 443, 454, and 456 nm, respectively. For the VS-LED and DT-LED with tensile stresses as compared with LS-LED, longer wavelengths are observed. On the contrary, the LS-LED displayed a shorter wavelength for containing the compressive stress. Note that, these LEDs were fabricated using the sample wafer. It suggested that the epilayers presented a compressive strain after MOCVD growth and then exhibited a tensile strain after epilayer transferring. The results are in good agreement with those of Raman measurement. Moreover, it is worthy to mention that the EL peak wavelengths of these three GaN-on-Si based LEDs are firstly shifted to the shorter wavelength (blue-shift) with increasing the injection current from 20 to 450 mA. As the injection current exceeds 450 mA, a red-shift is then appeared. In general, the blue-shift is attributed to the band-filling effect in the low injection current level and the red-shift is owing to the thermal effect [24, 25]. It is also found that the wavelength shift in LS-LED is more serious than that in VS-LED and DT-LED. The blue-shift formed at high injection current can be explained by the quantum-confined Stark effect, where the piezoelectric polarization fields are developed from the strained nature of the MQWs [26, 27]. Additionally, the red-shift can be explained by the thermal band-gap shrinkage due to the thermal effect with increasing the injection current, which leads to an increase in Joule heating. Obviously, although the Si substrate can play a role of the heat sink for the LS-LED, it also absorbs more light and heat by itself. This induces more Joule heating in the LS-LED as the injection current is more than 450 mA.

#202212 - $15.00 USD Received 28 Nov 2013; revised 3 Jan 2014; accepted 3 Jan 2014; published 10 Jan 2014

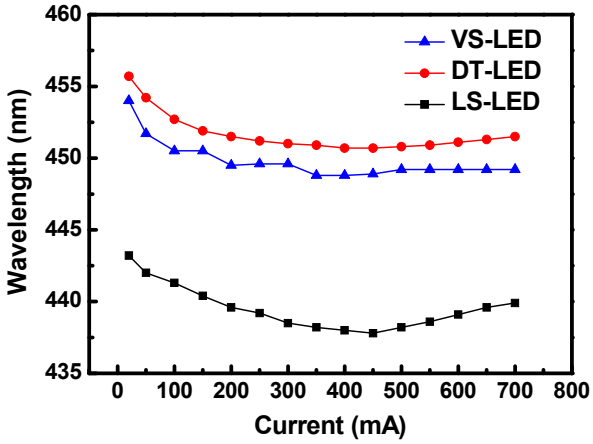

Fig. 4. Emission wavelength as a function of injection current for the LS-LED, DT-LED, and VS-LED.

On the other hand, typical optical properties including light output power and external quantum efficiency (EQE) of these three LEDs are also measured with varying the injection current, as shown in Fig. 5. It can be seen clearly that the light output powers of these LEDs increase linearly with increasing the injection current initially. At an injection current of 350 mA, the light output powers of LS-LED, DT-LED, and VS-LED are 60.02, 93.35 and 140.62 mW, respectively. The increments in output power (@ 350 mA) of VS-LED and DT-LED have reached to 134.29% and 55.54%, respectively, in comparison to that of LS-LED. Under a high injection current of 700 mA, the light output powers of LS-LED, DT-LED, and VS-LED are 90.88, 155.07, and 261.07 mW, respectively. It is found that the increments in output power (@ 700 mA) of VS-LED and DT-LED are further increased to 187.26% and 70.63%, respectively, as compared with that of LS-LED. The increasing rates of output power for VS-LED and DT-LED are both greater than that of LS-LED as the injection current is increased. It means the generated photons cannot only be reflected from the high-reflection mirror, but also escape from the roughened n-GaN surface, and consequently improve the light extraction [28–31]. In addition, it can be observed that the light output power of LS-LED is the worst one due to the absorption of downward photons by the Si substrate for no mirror fabrication.

Similarly, as shown in Fig. 5, the highest EQE of VS-LED could be expected due to its high output power as mentioned above. However, it can be seen that there are efficiency droops in EQE at all LEDs as the injection current is increased from 20 to 700 mA [32]. The efficiency droop can be defined as $[(EQE_{max}-EQE_{min})/EQE_{max}]$, where EQE_{max} and EQE_{min} denote the maximum and minimum efficiencies of LED, respectively. After calculation, EQE droops are determined to 29.33%, 35.99%, and 55.57% for VS-LED, DT-LED, and LS-LED, respectively. The efficiency droop is usually formed because of several factors, such as Auger recombination due to high carrier density, electron overflow owing to the polarization fields in the MQW region, and so on [33–35]. In this case, the efficiency droop is decreased from 55.57% in LS-LED to 29.33% in VS-LED. This difference could be ascribed to the thermal dissipation, effect of mirror, and fabrication of roughened surface in VS-LED. From the above analyses, it can be concluded that the VS-LED possesses the best device performance due to its current spreading, light extraction, and thermal dissipation.

#202212 - $15.00 USD Received 28 Nov 2013; revised 3 Jan 2014; accepted 3 Jan 2014; published 10 Jan 2014

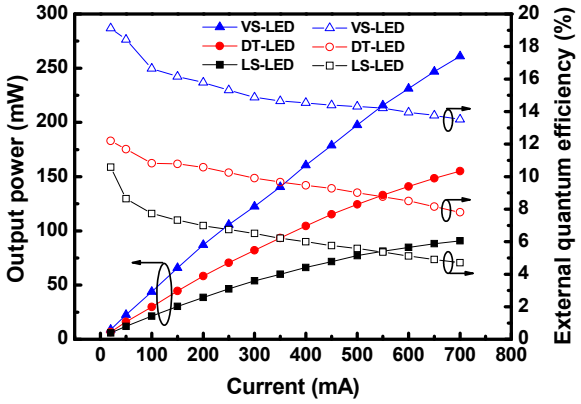

Fig. 5. Light output power and external quantum efficiency as a function of injection current for the LS-LED, DT-LED, and VS-LED.

Figure 6 shows the far-field radiation patterns (@ 350 mA) and emission images (@ 20 mA) of LS-LED, DT-LED, and VS-LED. From the far-field radiation patterns, it can be unsurprisingly found that the VS-LED possesses higher output intensity than that of DT-LED and LS-LED in almost full angle. This result is attributed to the effect of mirror, surface roughening, and good current spreading in vertical-type LED. The viewing angles of 129.1°, 128.7°, and 128.5° are measured for LS-LEDs, DT-LED, and VS-LED, respectively. However, the overall integrated area of EL intensity of DT-LED is still larger than that of LS-LED. It indicates that the enhancement in light intensity by adopting the high-reflection mirror and roughened u-GaN surface is more remarkable, which could be considered as a consequence of high light scattering efficiency.

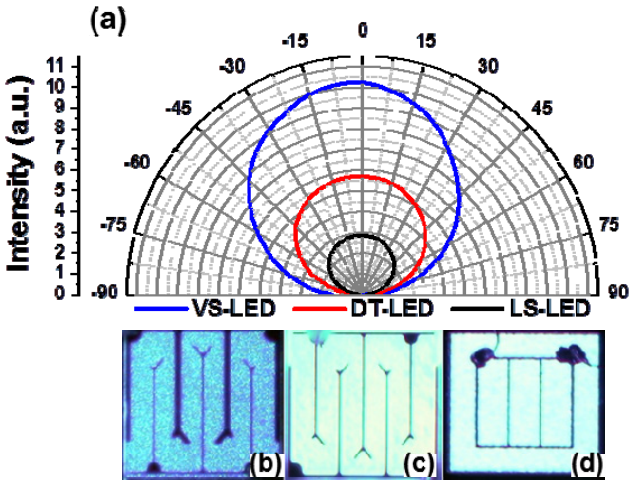

Fig. 6. (a) Far-field radiation patterns of the LS-LED, DT-LED, and VS-LED at the injection current of 350 mA. Emission images (@ 20 mA) of the (b) LS-LED, (c) DT-LED, and (d) VS-LED.

4. Conclusion

In conclusion, the performance of the GaN-based LEDs grown on Si(111) substrate is further improved by transferring the device to Si(100) substrate using the CLO and double-transfer techniques. With fabricating a vertical-type device, VS-LED achieves a higher output power of 261.07 mW at an injection current of 700 mA, which is 187.26% higher than that of LS-LED.

#202212 - $15.00 USD Received 28 Nov 2013; revised 3 Jan 2014; accepted 3 Jan 2014; published 10 Jan 2014

This high output is mainly attributed to the assistances of high-reflection mirror and roughened surface. Moreover, VS-LED also presents better performances in EQE, efficiency droop, far-field radiation, and epilayer stress. The EQE droop (@ 700 mA) of 29.33% observed in VS-LED is better than that of DT-LED (35.99%) and LS-LED (55.57%). The stress between Si and GaN epilayer can be effectively released after transferring the epilayer. It is a promising result for further development of GaN-on-Si based LEDs.

Acknowledgment

This work is supported by the National Science Council of the Taiwan, Republic of China under Contract No. NSC 100-2221-E005-092-MY3.

#202212 - $15.00 USD Received 28 Nov 2013; revised 3 Jan 2014; accepted 3 Jan 2014; published 10 Jan 2014